RSC Advances




ROYAL SOCIETY OF CHEMISTRY

www.rsc.org/advances

Cite this: DOI: 10.1039/c0xx00000x

www.rsc.org/xxxxxx

ARTICLE TYPE

# Enzymatic deacidification of the rice bran oil and simultaneous preparation of phytosterol esters-enriched functional oil catalyzed by immobilized lipase arrays

**Mingming Zheng,[a] Jiuxia Zhu,[b] Fenghong Huang,*[a,c] Xia Xiang [a], Jie Shi[a], Qianchun Deng,[a, c] Fangli Ma[c] and Yuqi Feng*[b]**

***Received (in XXX, XXX) Xth XXXXXXXXX 20XX, Accepted Xth XXXXXXXXX 20XX***
**DOI: 10.1039/b000000x**

**Abstract:** Rice bran oil (RBO) is a great and important vegetable oil resource, but usually contain high content of free fatty acids (FFAs). Phytosterol esters are functional lipids possessing hypocholesterolemic activity. In this study, *Candida rugosa* lipase (CRL) was immobilized on the octyl-functionalized ordered mesoporous silica (C8-OMMs) to obtain immobilized CRL arrays (CRL@C8-OMMs). The resulting CRL@C8-OMMs arrays showed much better thermal stability and reusability in comparison to free CRL. The deacidification and simultaneous preparation of functional oil rich in phytosterol esters (PEs) was successfully achieved by enzymatic esterification of high-acid RBO with phytosterol. The contents of FFAs and PEs were below 2.4% and above 84.7%, respectively. Repeated reaction tests indicated that CRL@C8-OMSs arrays could be used 11 times with 80.7% of its original catalytic activity still retained. The strategy could not only take advantage of the high-acid oils resources, but also product PEs-enriched functional oils.

## 1. Introduction

Worldwide rice production is around 600 million tons per year, 5-6% of which is bran[1]. The bran contains about 14% oil. The rice bran oil (RBO) has a balanced fatty acid profile and contains a lot of minor constituents with proven nutritional benefits such as γ-oryzanol, tocotrienols, tocopherols, and squalene[2]. However, owing to lipase hydrolysis of oil within the seeds, RBO may contain as much as 30% to 40% free fatty acids (FFAs), if the bran is not processed promptly after polishing from the rice grain. High-acid RBO is a great vegetable oil resource need to be utilized. The conventional refining process involves several steps (e.g., degumming, dewaxing, deacidification, bleaching, and deodorization) [3]. The high FFA content is responsible for greater oil refining loss and the darker color of processed oil produced by the conventional refining process[4], which could be a waste of high-acid oil resource. As an alternative, enzymatic refining is an effective approach to the deacidification of high-acid oil[5, 6]. Using the enzymatic esterification, FFAs could be converted to different acylglycerols, including monoacylglycerol (MAG), diacylglycerol (DAG), and triacylglycerol (TAG). Only a few reports showed the effectiveness of using glycerol, MG, and DG as esterifying agents to reduce the FFA level of RBO. Bhattacharyya et al. reported that enzymatic esterification was effective to reduce FFA in the RBO and produce oils with better quality[5]. However, there has been no report using any other esterifying agents.

Phytosterols have attracted great attention because they are known to have a hypocholesterolemic effect by lowering plasma total and low-density lipoprotein (LDL) cholesterol levels without affecting plasma high-density lipoprotein (HDL) cholesterol concentration7. Phytosterol esters (PEs), derived from phytosterols and inheriting all of the excellent properties of phytosterols mentioned above, have a much greater solubility in oils and a lower melting point as compared to the corresponding phytosterols[8,9]. Owing to these advantages, PEs are easily incorporated into a wide variety of diets and fat-based food products[7-9]. It is worth noting that the FFAs containing in high-acid RBO were usually used as the acyl donors for PEs preparation.

Enzymatic catalysis, which proceeds efficiently under mild conditions, produces fewer by-products, and benefits from the biocatalyst's high specificity, is attractive for the synthesis of PEs[8,10,11]. In order to enhance the operational activity and stability, most of lipases used in industrial processes were in the immobilized state[12-14]. Enzyme immobilization and biocatalysis process would benefit from more uniform and open porous networks structure that provide optimal mass diffusion and improved efficiency[15,16.] Among numerous possible carriers, ordered mesoporous/nanoporous materials (OMMs) with large pore sizes (>10 nm) have attracted considerable attention since they have large specific surface area, tunable porosity, low cytotoxicity, favorable mechanical properties and the ease with which their pore surfaces can be chemically modified[17-19].

The main objective of this study is to develop a strategy for enzymatic deacidification of high-acid oil and preparing of functional oil rich in PEs. The immobilized lipase arrays, which employ octyl-functionalized OMMs as carrier, were prepared, characterized and employed as the biocatalyst. Then, a green and convenient method was proposed for the one-pot enzymatic esterification of phytosterols with high acid-value RBO. To the best of our knowledge, enzymatic deacidification of high-acid

RBO using phytosterols as the esterifying agent and simultaneous production of the PEs-enriched RBO have not been reported.

## 2. Experimental

### 2.1 Chemicals and reagents.

Tetraethoxysilane (98%, TEOS) and *n*-octyltriethoxysilane (97%, C8-TEOS) were purchased from the Chemical Plant of Wuhan University (Wuhan, China). Isooctane, triethylamine and, 1,3,5-trimethylbenzene (TMB) and other solvents were purchased from Sinopharm Chemical Reagent (Shanghai, China) and were of analytical reagent grade. Purified water was obtained with Millipore water purification equipment (Bedford, USA).

*Candida rugosa* lipase (CRL, lyophilized powder, Type VII, 700 U $mg^{-1}$ solid), Triblock copolymers EO106PO70EO106 (Pluronic F127) and p-nitrophenyl palmitate (p-NPP) were purchased from Sigma-Aldrich (St. Louis, USA); Phytosterols (β-sitosterol (89.0%), campesterol (8.9%), stigmasterol (2.1%)) were purchased from Vita-Solar Biotechnology Co., Ltd. (Xi'an, China); oleic acid (90%) were purchased from Aladdin Industrial Corporation (Shanghai, China); Crude rice bran oil containing different content of FFAs was purchased from Yinhe Pharmaceutic Industry (Zhejiang, China).

### 2.2 Preparation of octyl-functionalized ordered mesopore silica (C8-OMMs).

The OMMs was prepared according to previously reported method with a little modification[15]. Briefly: 0.50 g triblock copolymers EO106PO70EO106 (Pluronic F127), 0.60 g 1,3,5-trimethylbenzene (TMB) and 1.25 g of KCl were dissolved in 50 mL of 1 M HCl at 15 ± 0.1°C. After 1 h stirring, 2.08 g tetraethyl orthosilicate (TEOS) was added to this solution. The reactant molar ratio of F127/KCl/TEOS/TMB/HCl/$H_2O$ was 0.00147/0.62/0.37/0.185/1.85/100. After stirring for 24 h at 15 ± 0.1 °C, the mixture was transferred into an autoclave and heated at 200 °C for 24 h. The product was obtained after filtration and dried at room temperature in air.

The organic templates were removed by microwave digestion as described by Tian et al[20]. The detailed process was conducted as follows: 0.3 g OMMs sample was mixed with 2 mL 30% $H_2O_2$ and 6 mL 15 M $HNO_3$ in a 30 mL Teflon sample vessel. The system was operated at approximately 800 W. The operation temperature of the digestion process was maintained at 170 °C for 10 min. The sample after microwave digestion was washed by water for three times and then dried for further use.

The octyl bonded OMMs were prepared by adding 2.65 g of C8-TEOS, 66 μL triacetate abdominal, 4.0 g of dried OMMs in 20 mL of anhydrous toluene in a 100 mL hydrothermal reactor, and the mixture was hydrothermal treated at 130 °C for 20 h. The resulting material was filtered through a sintered glass funnel (G3) and then washed with several aliquots of anhydrous ethanol and water in sequence. After being dried overnight at 80 °C under vacuum condition, the C8-OMMs were obtained.

### 2.3 Immobilization of lipase on C8-OMMs

Immobilization of lipase on the C8-OMMs (1.0 g) via adsorption was studied in phosphate buffer (25 mL, 100 mM, pH 7.0). The effect of initial lipase concentration on the immobilization efficiency was studied at different initial lipase concentrations in the range of 1.1 to 6.6 mg $mL^{-1}$. The immobilization experiments were conducted at 30 °C for different time with continuous stirring. After the immobilization was done as described above, the CRL@C8-OMMs arrays were separated from the enzyme solution and washed with buffer solution and acetone, respectively. The amount of immobilized lipase was obtained by using the following equation (1):

$$Q=[(C_0-C)V]/M \quad (1)$$

where Q is the amount of lipase immobilized onto OMMs (mg $g^{-1}$); $C_0$ and C are the concentrations of the lipase in the initial and final solutions (after combining wash solution), before and after immobilization, respectively (mg $mL^{-1}$); V is the volume of the aqueous solution (mL); M is the mass of the beads (g). The amount of protein in medium and wash solutions was determined by the Bradford method [21].

### 2.4 Measurement of free and immobilized CRL activities

The enzymatic activities of free and immobilized CRL were measured by the detection of the p-nitrophenol which comes from the hydrolysis of p-nitrophenyl palmitate (p-NPP)[22]. Free lipase or immobilized lipase was added to a mixture of 1 mL of 0.5% (w/v) p-NPP solution and 1 mL of 0.05 M PBS (pH 7.0) and incubate for 5 min at 30 °C. The reaction was terminated by adding 2 mL of 0.5 N $Na_2CO_3$ followed by centrifuging for 10 min (10,000 rpm). The supernatant of 0.5 mL was diluted 10-folds with distilled water, and measured at 410 nm in a UV/VIS spectrophotometer (Beckman DU-800, Fullerton, USA). One unit (U) of enzyme activity was defined as the amount of enzyme which catalyzed the production of 1 mmol p-nitrophenol per minute under the experimental conditions. The relative activity (%) was the ratio between the activity of every sample and the maximum activity of sample.

The effects of temperature on lipase activity were performed by the incubation for 0.5 h of the immobilized or free CRL at various temperatures (20 °C-70 °C). The thermal stability assays were performed by the incubation for different time (0-240 min) of the immobilized or free CRL at 55 °C. After cooling to room temperature, the activity of enzyme was measured under standard conditions (pH 7.0, 37 °C) as described above. Residual activities were calculated as the ratio of the activity of enzyme measured after incubation to the maximal activity of the enzyme.

### 2.5 One-Pot Enzymatic esterification of phytosterol with high-acid RBO

The following esterification conditions were used: 100 mmol $L^{-1}$ high-acid RBO (different batch of RBO with FFAs content in the range of 10%-40%), 100-500 mmol $L^{-1}$ phytosterols, immobilized lipase (CRL@C8-OMMs arrays, 20 mg $mL^{-1}$), and solvent (isooctane, 10 mL) were added into an Erlenmeyer flask. The

solvent had, in advance, been dehydrated with 15% (w/w) molecular sieves 3 Å for at least 24 h. The vial was placed in a shaking incubator at 55 °C with a shaking speed of 180 rpm for 2 h. The bioconversion was monitored periodically by GC to confirm production. The bioconversion was calculated from the ratio between the measured concentration of PEs and the expected concentration assuming complete reaction. Following the lipase-catalyzed esterification, the product was placed to the refrigerator (4°C) for 1 h, then the excess phytosterols, immobilized lipase and molecular sieves were filtered from the mixture. The functional oil was obtained after rotary evaporation to remove reaction solvent.

### 2.6 Qualitative and quantitative analysis of PEs and FFAs

The composition of the crude products was analyzed by GC. An Agilent 6890 Series II gas chromatograph (Hewlett-Packard Co., Avondale, PA, USA), equipped with a flame ionization detector (FID) and a fused silica capillary column (DB-5 HT, 15.0 m×320 μm×0.10 μm, Agilent Technologies., Deerfield, IL, USA) was used. The carrier gas was nitrogen and the total gas flow rate was 3.5 mL $min^{-1}$. The injector and detector temperatures were maintained at 320°C and 350°C, respectively. The oven temperature was held at 210°C for 2.0 min, then increased to320 °C at a rate of 10°C $min^{-1}$ and held for 15 min, then increased to 380°C at a rate of 10°C $min^{-1}$, finally it was held at 380°C for another 5 min. The injection volume was 1 μL in split mode. The split ratio was 50:1. With the GC operation conditions above, the retention times of each compound were as follows: FFAs (before 2 min), β-sitosterol (4-6 min), and phytosterols esters (11 min-13 min).

The degree of esterification (%) of phytosterols with FFAs to form PEs was calculated from the GC profile of reactants using the following Eq. (2):

$$\text{Degree of esterification (DE, \%)} = \frac{B}{B+1.63\times A}\times 100 \quad (2)$$

Where A = peak area of total phytosterols (campesterol+ stigmasterol+β-sitosterol); B = peak area of total PEs of FFAs. 1.63 = ratio of average molecular weight of total PEs to average molecular weight of total phytosterols.

The FFAs content was determined according to the international standard (ISO 660:2009 (E))[23]. Briefly, 3.0 g of sample dissolved in organic solvent (ether: ethanol=1:1, v/v), is titrated with a potassium hydroxide (KOH) solution with phenolphthalein as a color indicator.

## 3. Results and discussions

### 3.1 Characterization of the OMMs and CRL@C8-OMMs arrays

The morphology and structure of the as-synthesized spheres were investigated by scanning electron microscopy (SEM) and transmission electron microscopy (TEM). The OMMs exhibit monodisperse, uniform and hexagon morphologies with an average diagonal length of 8.0-10.0±0.5 μm, thickness of 2.0-3.0±0.5 μm (Fig. 1a, 1b).

High-resolution SEM (Fig. 1c) images show that hexagonal arrays of uniform cages (about 25 nm) are found throughout the surface of the hexagonal prisms, indicating that both the top and side faces of the hexagonal prisms are enclosed by {1,1,1} facets [15]. From the TEM images (Fig. 1d), it can be seen that the average diameter of the ordered mesoporous is about 20 nm. The lipase was immobilized in the uniform hexagonal arrays via hydrophobic interaction, forming a immobilized lipase arrays. Excellent biocatalysts reported in literatures are enzymes, which are spreading over the internal surface of porous materials, acting as carriers or supports[17]. In this study, the catalysis processes could benefit from the uniform and ordered three-dimensional large mesoporous networks of OMMs as that could provide optimal mass diffusion.

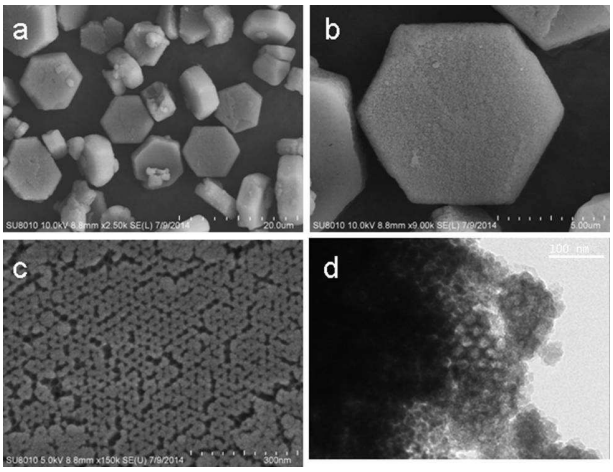


**Fig. 1** SEM (a-c) and TEM (d) images of the OMMs carrier.

The $N_2$ adsorption-desorption isotherms and pore size distributions of OMMs, C8-OMMs and CRL@C8-OMMs arrays were measured (Figure S1a, S1b). N2 sorption isotherms of OMMs and C8-OMMs (Figure S1a) exhibited a typical type IV curve with a H1-type hysteresis loop at a relative pressure (p/p0) range of 0.6-1.0, The huge hysteresis loop in the higher relative pressure (>0.4) indicated the presence of a large amount of mesopores and macropores. As listed in Table 1, the surface area decreased gradually in the order: OMMs>C8-OMMs>CRL@C8-OMMs arrays; and the pore volume also decreased in the same order. Compared with OMMs, the pore volumes of C8-OMMs and CRL@C8-OMMs arrays decreased sharply, while the pore size distribution showed little change (Figure S1b). This indicated that octyl-functional groups had been introduced into the cavities of OMMs, and moreover, the CRL had been immobilized in the cages of the OMMs with a bottle-neck structure. Correspondingly, the cage and entrance size of OMMs calculated from the adsorption branch and desorption branch using the Barrett-Joyner-Halenda (BJH) method reveals a distribution centered at 25.8 nm and 16.7 nm, respectively. The CRL was adsorbed inside the larger cages (20.8 nm) of the C8-OMMs. The cages not only offer a suitable micro-environment for the CRL but also decrease the leakage of the CRL through the smaller window (13.4 nm).

To confirm that lipase *Candida rugous* was immobilized on the C8-OMMs, the FT-IR spectra of OMMs, C8-OMMs, CRL@C8-OMMs arrays and native lipase were investigated (Fig. 2). For OMMs, the bands at 804 and 1089 $cm^{-1}$ could be assigned to the symmetric stretching vibration of Si-O and antisymmetric stretching vibration of Si-O-Si[24]. For octyl-functionalized OMMs (C8-OMMs), the peaks at 2856 $cm^{-1}$ and 2924 $cm^{-1}$ could be assigned to the C-H symmetric and anti-symmetric stretching vibrations. For the native lipase, the peaks observed in the regions 1407 and 1535 $cm^{-1}$ corresponded to the bending vibrations of -C-H and -N-H[25]. The -C-H and -N-H absorption peaks observed in the FT-IR spectrum of CRL@C8-OMMs arrays confirmed that *Candida rugous* lipase had been successfully immobilized on C8-OMMs arrays.

**Table 1.** Surface area ($S_{BET}$), cage size, entrance size and pore volume ($Vp$) of the OMMs, C8-OMMs and CRL@C8-OMMs[a]

| Sample | $S_{BET}$ ($m^2$ $g^{-1}$) | Cage[b] (nm) | Entrance[c] (nm) | $Vp$ ($cm^3$ $g^{-1}$) |
|---|---|---|---|---|
| OMMs | 196.5±3.9 | 25.8±0.8 | 16.7±0.5 | 1.02±0.3 |
| C8-OMMs | 164.8±3.5 | 20.8±0.6 | 13.4±0.4 | 0.84±0.3 |
| CRL@C8-OMMs | 149.7±3.2 | 15.5±0.5 | 12.2±0.3 | 0.73±0.2 |

[a]Values are means ± standard deviation, n = 3.
[b] Cage size calculated from the adsorption branch.
[c] Entrance size calculated from the desorption branch.

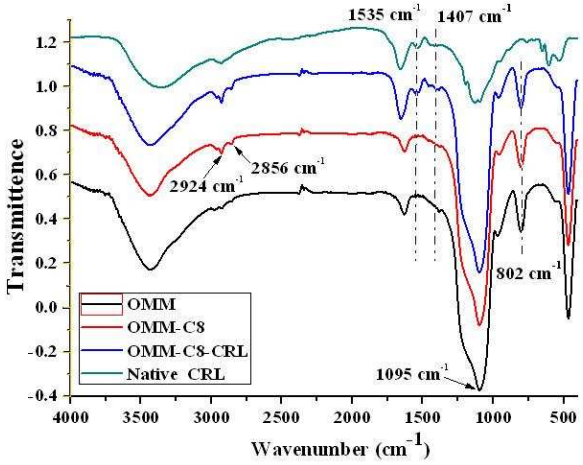


**Fig. 2** FT-IR spectra of OMMs, C8-OMMs, CRL@C8-OMMs and native CRL.

### 3.2 Lipase immobilization on the C8-OMMs carriers

The initial concentration of enzyme solution employed for the immobilization is another important factor for the immobilization process. It affects not only the adsorption amount of the lipase on carrier but also the activity of immobilized lipase[26]. There was a high correlation coefficient between the lipase amount in the C8-OMMs and the initial lipase concentration from 1.1 to 6.6 mg $mL^{-1}$ (Fig. 3). The effect of the lipase concentration on the lipase amount immobilized on the carrier and the apparent activity was evaluated. The maximum specific activity of the immobilized lipase increased to 501.3 U $g^{-1}$ as the lipase amount in the carrier increased to 92.3 mg $g^{-1}$. However, the specific activity obviously decreased as the lipase amount on the C8-OMMs carrier further increased. The suppression of the specific activity might be ascribed to the conformational changes in the lipase. At high lipase amount in the carrier, mass-transfer limitations lead to reduced activity[27]. Moreover, the lipase tends to be packed by forming more than monolayer on the surface of the carrier, causing the decrease in the activity[26]. Therefore, the lipase concentration of 4.5 mg $mL^{-1}$, which corresponds to 92.3 mg $g^{-1}$ of lipase amount on C8-OMMs carrier, was selected as optimum condition.

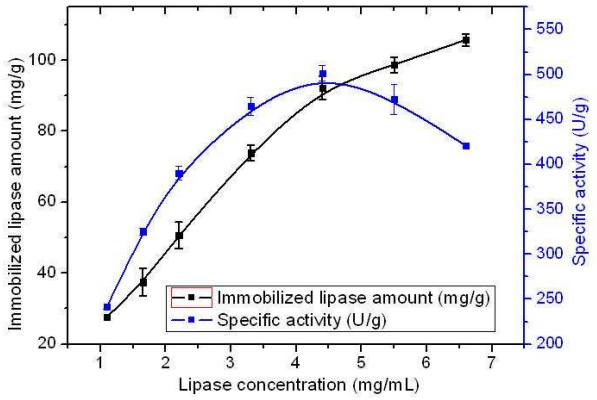


**Fig. 3** Effect of initial protein concentration on protein amount in the CRL@C8-OMMs arrays (left) and specific activity of the CRL@C8-OMMs arrays (right). Each experiment date from Fig. 3 to Fig. 8 was duplicated for three times. The standard deviations were shown as error bars in each Figure.

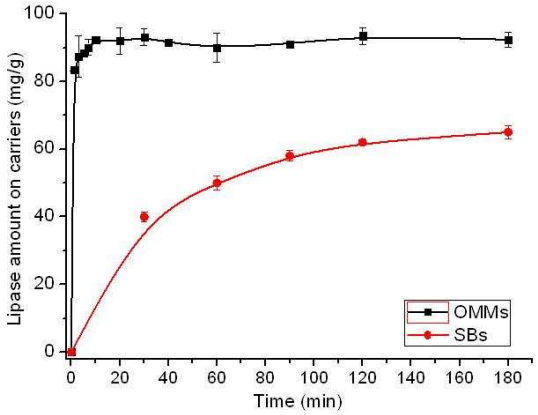


**Fig. 4** Time course of lipase immobilization on OMMs arrays and silica beads (SBs).

It is crucial that the adsorption of enzyme be controllable for the successful preparation of immobilized enzyme. For comparison with the ordered mesoporous material-based immobilized lipase, silica beads (10 μm, 280 $m^2$ $g^{-1}$ and 10 nm mesoporous size) was chosen as a host material. Lipase *Candida rugous* was immobilized on octyl-functionalized silica beads (C8-SBs) and C8-OMMs by adsorption (the immobilized lipases were named CRL@C8-SBs and CRL@

C8-OMMs arrays, respectively). The loading amounts and loading times of the lipase on the different carriers were obtained and are summarized in Fig. 4. These two carriers adsorbed CRL well, and the adsorption amounts and equilibrium times were measured to be 65.2 mg $g^{-1}$ and 180 min for SBs and 92.3 mg $g^{-1}$ and 10 min for C8-OMMs, respectively. The immobilized enzyme amount and the immobilized speed on C8-OMMs were 1.4-fold and 18-fold larger than those on C8-SBs, respectively, indicating that C8-OMMs arrays with larger ordered pore sizes and higher pore volumes are much better candidates for adsorption immobilization of enzyme.

### 3.3 Thermal effects on activity and stability of free CRL and CRL@C8-OMMs arrays

The effect of temperature on lipase activity was expressed as percentage of the maximum activity, which was investigated in phosphate buffer (0.1 M, pH 7.0) in the range of 20-70°C after 5 min of reaction. The activity profiles of free and immobilized CRL at different temperatures are represented in Fig. 5a. As the temperature increases above 30°C, the relative activity of the free lipase decreased much greater than the CRL@C8-OMMs. At 60°C the free CRL retained only 22.6% residual activity while immobilized lipase retained 65.5% of its initial activity. Similarly at 70°C the free CRL retained only 4.5% residual activity while immobilized CRL was found to retain 53.3% of its initial activity. It might be due to the creation of conformational limitation on the lipase movement in the cage of C8-OMMs arrays as a result of hydrophobic interaction between the lipase and the carriers[28].

Thermal stability experiments were carried out with free and immobilized CRL, which were incubated in the absence of substrate at 55°C. As shown in Fig. 5b, it is observed that the free CRL has lost half of its activity within only 30 min. In contrast, CRL@C8-OMMs arrays still retained its initial activity of 78.9% after 120 min of heat treatment at 55°C, proving enhanced thermostability of the carriers. This is attributed to the stabilizing effect of the C8-OMMs matrix with large ordered mesoporous and the hydrophobic interaction between CRL and carriers, which prevents extensive conformational changes typical of thermal denaturation[29]. The ability to retain enzyme activity at high temperatures provides a number of advantages such as improving substrate solubility, reaction rate and conversion, thereby expanding the range of applications of enzymatic synthesis.

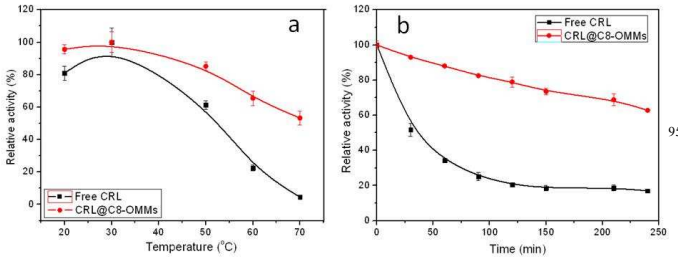


**Fig. 5** Effect of temperature on the activity (a) and stability (b) of free CRL and CRL@C8-OMMs arrays.

### 3.4 Enzymatic esterification of phytosterols with high-acid RBOs

The molar ratio of FFAs in high-acid RBO to phytosterols effects both the conversion to PEs and the deacidification efficiency. The molar ratio of FFAs to phytosterols was investigated from 1:1 to 1:5. With the molar ratio of FFA to phytosterols increasing from 1:1 to 1:5, as shown in Figure 6, the conversions decreased from 95.2% to 85.4% slowly, and moreover, the FFAs content of RBO was decreased from 12.9% to 1.4% sharply. The result indicated that the enzymatic esterification of phytosterols with high-acid RBO could not only preparation of PEs with high conversion, but also consumes the residual FFAs. Most of the phytosterols were not soluble in the solvent at higher molar ratio, which was responsible for the low conversion at relative high phytosterols concentration. In addition, it may not only change the catalytic environment and the active site of CRL@C8-OMMs arrays, but also increase the viscosity of the reaction solvent and thus decrease the mass transfer rate at higher molar ratio[30]. Considering the extent of esterification and the residue FFA contents of the process, the mole ratio of 1:4 was selected for the RBO containing 20.9% FFA.

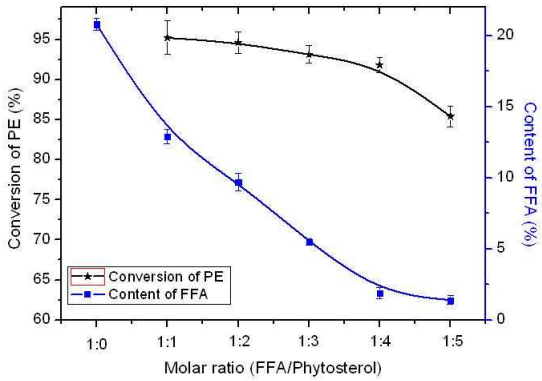


**Fig. 6** Effect of molar ratio of FFAs to phytosterols on conversion to PEs and FFAs content in RBO. Reaction conditions: 20.9% FFAs content in RBO, 100 mmol $L^{-1}$ of RBO, 20 mg $mL^{-1}$ of CRL@C8-OMMs array in 10 mL isooctane, 180 rpm and 55°C.

Under the optimized conditions, the esterification of phytosterols with four high-acid RBOs containing FFAs content between 10.4%-40.7% was investigated. As listed in Table 2, the final FFAs content and deacidification efficiencies were in the ranges of 0.8%-2.3% and 92.3%-94.5%, respectively. The RBO samples which FFAs content below 20.9% have reached the Chinese national standard of the RBO (FFAs content<1.5%, GB 19112-2003) after enzymatic deacidification by this strategy without further processing. The phytosterol and PEs content in four different functional oils was in the ranges of 2.5%-3.8% and 84.7%-86.0%, respectively. GC analysis results showed that the peaks of PEs were observed in functional oil obviously (Fig. 7). The peaks of phytosterols and FFAs in functional oil were almost disappeared, which prove that the enzymatic esterification ratio was quite high (≥91.2%). The results suggest that CRL@C8-OMMs arrays could be used to catalyze the esterification of phytosterols with high-acid RBOs with relatively high conversion. This might be ascribed to the fact that lipases prefer to adsorb on hydrophobic supports, involving the adsorption of the hydrophobic areas surrounding the active center and leaving the active site fully exposed to the reaction medium[16]. This

strategy could not only effectively deacidify the high-acid RBOs by using the phytosterols as the esterifying agents, but also produce PEs which was abundant in functional oil.

**Table 2.** Deacidification effect and esterification conversion using different high-acid RBOs as the raw material[a]

| High-acid RBOs | $C_{FFA0}$[b] (%) | $C_{FFAt}$[c] (%) | Deacidification efficiency (%) | $C_P$[d] (%) | $C_{PE}$[e] (%) |
|---|---|---|---|---|---|
| 1 | 10.4±0.4 | 0.8±0.02 | 92.3±1.1 | 3.8±0.12 | 84.7±1.3 |
| 2 | 20.9±0.8 | 1.4±0.03 | 94.4±1.3 | 3.5±0.11 | 84.9±1.2 |
| 3[f] | 30.8±1.2 | 2.1±0.04 | 93.0±1.5 | 2.8±0.11 | 85.5±1.8 |
| 4[f] | 40.7±1.4 | 2.3±0.05 | 94.5±1.6 | 2.5±0.10 | 86.0±2.1 |

[a]Values are means ± standard deviation, n = 3. [b] $C_{FFA0}$: the FFAs content in initial high-acid RBOs; [c] $C_{FFAt}$: the FFAs content in final functional oils; [d] $C_P$: the phytosterol content in final functional oils; [e] $C_{PE}$: the PEs content in final functional oils; [f]The molar ratio of FFAs to phytosterols was 1:3 and 1:2.5 for No.3 and No.4 high-acid RBOs, respectively.

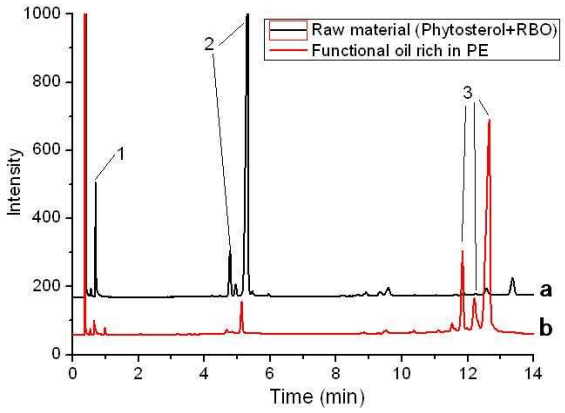


**Fig. 7** Gas chromatograms of raw material (RBO and phytosterols mixture) (a) and responding functional oils (b). Peaks: (1) FFAs; (2) phytosterols; (3) phytosterol esters.

The reusability of immobilized enzyme is rather important for its practical application. At the end of each reaction batch, the CRL@C8-OMMS arrays were washed with isooctane to remove any substrate and product retained on the support and then lyophilized. The CRL@C8-OMMs arrays were consecutively reused after each reaction cycle. The effect of repeated CRL@OMMs arrays use on the conversion of PEs was investigated (Fig. 8). It was observed that CRL@OMMs arrays kept excellent activity after 11 reuses as the conversion to PEs still remained 80.7%. This result confirmed that the immobilized CRL on C8-OMMs allowed not only excellent activity, but also satisfactory reusability in 11 reaction cycles. Benefit from the large ordered mesoporous cage structure of the OMMs arrays, the excellent enzymatic activity and fine reproducibility can be attributed to the better mass transfer of substrates and products and the robust immobilization ability of the OMMs arrays without affecting the active sites and subunits of CRL, respectively. In addition, the cages of OMMs arrays could protect the CRL from mechanical inactivation caused by shaking. The advantages mentioned above make it possible for the CRL@C8-OMMs arrays to be applied as an efficient biocatalyst in industry.

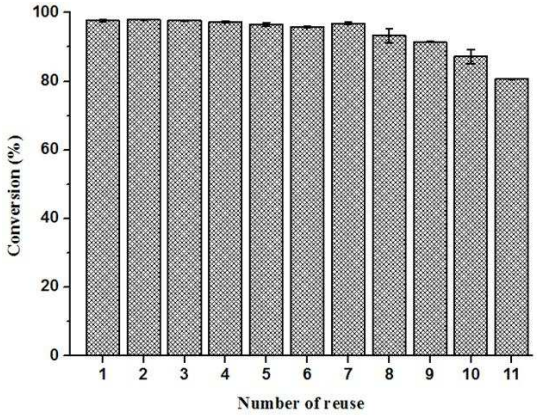


**Fig. 8** Reuse of CRL@C8-OMMs arrays for esterification of phytosterols. The reaction time was 2 h for each reaction cycle. Effect of molar ratio of FFAs to phytosterol is 1:4. Other reaction conditions were the same as those listed in Fig. 6.

## 4. Conclusions

In conclusion, the adsorption of CRL in the cages of C8-OMMs resulted in a highly stable and active immobilized lipase arrays. When CRL@C8-OMMs arrays were adopted as a biocatalyst, the preparation of RBO rich in PEs with low FFAs content by enzymatic esterification was successfully achieved. The CRL@C8-OMMs arrays could be used 11 times without loss its original catalytic activity. Benefit from these desired characteristics, this approach of immobilized lipase arrays could be applied in high-value utilization of the high-acid value oil resource, and might be employed to realize the immobilization of other enzymes with improved stability and catalytic activity.

## Acknowledgements

This work was supported by the National Natural Science Foundation of China (31371843, 3110353), the youth talents development program of Hubei province, the Earmarked Fund for China Agriculture Research System (CARS-13) and the Director Fund of Oil Crops Research Institute (1610172014006).

## Notes and references

[a]Oil Crops Research Institute, Chinese Academy of Agricultural Sciences, Hubei Key Laboratory of Lipid Chemistry and Nutrition, Wuhan 430062, China
[b]Key Laboratory of Analytical Chemistry for Biology and Medicine (Ministry of Education), Department of Chemistry, Wuhan University, Wuhan 430072, China
[c]Functional Oil Laboratory Associated by Oil Crops Research Institute , Chinese Academy of Agricultural Sciences and Infinite (China) Co., LTD., Guangzhou 51000, China
†Electronic Supplementary Information (ESI) available: Characterization of the immobilized lipase. See DOI:

1. J. Mehran, M. Alizadeh, M. Pirozifard, A. Qudsevali, *LWT-Food Sci. Technol.* 2008, **41**, 1892-1898.

2. W. Wang, J. Guo, J. N. Zhang, J. Peng, T. X. Liu, Z. H. Xin, *Food Chem.* 2015, **171**, 40-49.
3. C. E. C. Rodrigues, C. B. Goncalves, E. C. Marcon, E. A. C. Batista, A. J. A. Meirelles, *Sep. Purif. Technol.* 2014, **132**, 84-92.
4. Z. L. Song, Y. F. Liu, Q. Z. Jin, L. Li, X. G. Wang, J. H. Huang, R. J. Liu, *Appl. Biochem. Biotech.* 2012, **168**, 364-374.
5. B. K. De, D. K. Bhattacharyya, *J. Am. Oil Chem. Soc.* 1999, **76**, 1243-1246.
6. J. H. Lee, F. Yu, P. L. Vu, M. S. Choi, C. C. Akoh, K. T. Lee, *J. Food Sci.* 2007, **72**, 163-167.
7. Z. Y. Chen, K. Y. Ma, Y. T. Liang, C. Peng, Y. Y. Zuo, *J. Funct. Foods* 2011, **3**, 61-69.
8. B. H. Kim, C. C. Akoh, *Food Chem.* 2007, **102,** 336-342.
9. Z. Tan, K. Le, M. Moghadasian, F. Shahidi, *Food Chem.* 2012, **134**, 2097-2104.
10. M. M. Zheng, Y. F. Lu, H. Huang, L. Wang, P. M. Guo, Y. Q. Feng, Q. C. Deng, *J. Agric. Food Chem.* 2013, **61**, 231-237.
11. M. M. Zheng, Y. Lu, L. Dong, P. M. Guo, Q. C. Deng, W. L. Li, Feng, Y. Q. Huang, F. H. *Bioresource Technol.* 2012, **115,** 141-146.
12. N. Arifin, S. P. Koh, L. Kamariah, C. P. Tan, S. A. Y. Mohd, O. M. Lai, *Food Bioprocess Tech.* 2012, **5**, 216-225.
13. L.A. Lerin, A. Richetti, R. Dallago, H. Treichel, M. A. Mazutti, J. V. Oliveira, O. A. C. Antunes, E. G. Oestreicher, D. Oliveira, *Food Bioprocess Tech.* 2012, **5**, 1068-1076.
14. R. Chopra, N. K. Rastogi, K. Sambaiah, *Food Bioprocess Tech.* 2011, **4**, 1153-1163.
15. G. C. Ma, X. Q. Yan, Y. L. Li, L. P. Xiao, Z. J. Huang, Y. P. Lu, J. Fan, *J. Am. Chem. Soc.* 2010, **132**, 9596-9597.
16. Sun, J. M.; Zhang, H.; Tian, R. J.; Ma, D.; Bao, X. H.; Su, D. S.; Zou, H. F. *Chem. Commun.* 2006, **12**, 1322-1324.
17. M. Hartmann, *Chem. Mater.* 2005, **17**, 4577-4593.
18. M. Hartmann, X. Kostrov, *Chem. Soc. Rev.* 2013, **42**, 6277-6289.
19. S. Kataoka, Y. Takeuchi, A. Harada, M. Yamada, A. Endo, *Green Chem.* 2010, **12**, 331-337.
20. B. Z. Tian, X. Y. Liu, C. Z. Yu, F. Gao, Q. Luo, S. H. Xie, B. Tu, D. Y. Zhao, *Chem. Commun.* 2002, **11**, 1186-1187.
21. M. Y. Arica, H. Soydogan, G. Bayramoglu, *Bioproc. Biosyst. Eng.* 2010, **33**, 227-236.
22. S. H. Chiou,; W. T. Wu, *Biomaterials* 2004, **25**, 197-204.
23. International standard (ISO 660:2009 (E)): animal and vegetable fats and oils—determination of acid value and acidity. Switzerland
24. L. Y. Xia, M. Q. Zhang, C. E. Yuan, M. Z. Rong, *J. Mater. Chem.* 2011, **21**, 9020-9026.
25. L. Zhu, X. Y. Liu, T. Chen, Z. G. Xu, W. F. Yan, *Appl. Surf. Sci.* 2012, **258**, 7126-7134.
26. D. S. No, T. T. Zhao, J. S. Lee, I. H. Kim, *J. Agric. Food Chem.* 2013, **61**, 8934-8940.
27. B. C. Koops, E. Papadimou, H. M. Verheij, A. J. Slotboom, M. R. Egmond, *Appl. Microbiol. Biot.* 1999, **52**, 791-796.
28. Y. Kuwahara, T. Yamanishi, T. Kamegawa, K. Mori, M. Che, H. Yamashita, *Chem. Commun.* 2012, **48**, 2882-2884.
29. J. Lee, H. B. Na, B. C. Kim, J. H. Lee, B. Lee, J. H. Kwak, Y. Hwang, J. G. Park, M. B. Gu, J. Kim, J. Joo, C. H. Shin, J. W. Grate, J. Kim, *J. Mater. Chem.* 2009, **19**, 7864-7870.
30. J. A. Laszlo, K. O. Evans, *J. Mol. Catal. B: Enzym.* 2009, **58**, 169-174.

# Enzymatic deacidification of the rice bran oil and simultaneous preparation of phytosterol esters-enriched functional oil catalyzed by immobilized lipase arrays

**Mingming Zheng,[a] Jiuxia Zhu,[b] Fenghong Huang,*[a,c] Xia Xiang [a], Jie Shi[a], Qianchun Deng,[a, c] Fangli Ma[c] and Yuqi Feng*[b]**

[a]Department of Product Processing and Nutriology, Institute of Oil Crops Research, Chinese Academy of Agricultural Sciences, Hubei Key Laboratory of Lipid Chemistry and Nutrition, Ministry of Agriculture Key Laboratory of Oil Crops Biology, Wuhan 430062, China.

[b]Key Laboratory of Analytical Chemistry for Biology and Medicine (Ministry of Education), College of Chemistry and Molecular Sciences, Wuhan University, Wuhan 430072, China

[c]Functional Oil Laboratory Associated by Oil Crops Research Institute, Chinese Academy of Agricultural Sciences and Infinite (China) Co., LTD., Guangzhou 51000, China

Novel ordered mesoporous silica immobilized lipase arrays are described for enzymatic deacidification of the high-acid rice bran oil and simultaneous preparation of phytosterol esters-enriched functional oil.